

# A Novel Concept of High Voltage Auxiliaries and its Feasibility Study on Blower Motors

Satoshi Shiraki, Hiroyasu Kudo, Masakazu Tago, Akira Yamada, Shigeki Takahashi and Atsuyuki Hiruma

**Abstract** Hybrid/Electric Vehicles are expected to be one of the solutions for energy and environmental problems. Up to Now, low power automotive electronics have operated under a battery voltage of 12 V and a large current of more than 10 A. Because of this high current, the power electronic circuits cause substantial losses of power through wire harnesses, a DC/DC converter, semiconductors, and so on. In this paper, we have proposed a novel concept of high voltage auxiliaries, which replaces the 12 V loads with the high voltage loads driven directly by the high voltage battery. It is assured that the power efficiency of the high voltage test system is as high as 94 %, which is at least 10 % higher than that of conventional 12 V blower motor systems.

**Keywords** Blower motor · Fuel Economy · High Voltage Auxiliary · Inverter Efficiency · Micro-Inverter IC

## 1 Introduction

Hybrid/Electric Vehicles are expected to be one of the solutions for energy and environmental problems [1]. The power supply system equipped on Hybrid/Electric Vehicle has a dual voltage battery, which consists of a high voltage battery (100–430 V) [2] and a 12 V battery connected through the step down DC/DC converter charged from the high voltage battery. Up to Now, low power automotive electronics have operated under a battery voltage of 12 V and a large

---

F2012-D02-018

---

S. Shiraki (✉) · H. Kudo · M. Tago · A. Yamada · S. Takahashi · A. Hiruma  
Denso Corporation, Kariya, Japan  
e-mail: SATOSHI\_SHIRAKI@denso.co.jp

current of more than 10 A. Because of this high current, the power electronic circuits cause substantial losses of power through wire harnesses, a DC/DC converter, semiconductors, and so on. In this paper, we have proposed a novel concept of high voltage auxiliaries, which replaces the 12 V loads with the high voltage loads driven directly by the high voltage battery.

The purpose of replacing the 12 V loads with the high voltage loads is to achieve higher efficiency using fewer electric parts, for better fuel economy. Therefore the most important points of the concept are as follows.

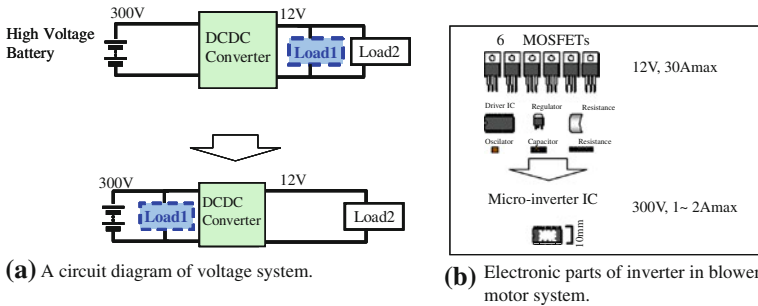
1. High power automotive electronics are generally controlled with a sinusoidal waveform current. Typically, they are controlled by vector controlled sinusoidal drives, which require a high performance Central Processing Unit (CPU). A sensor less sinusoidal wave drive technology has been developed for low power electronics, which maximizes the power by controlling the phase difference between the motor voltage and the motor current without using a high performance CPU.
2. Low power automotive electronics, blower motors for example, operate under a battery voltage of 12 V and a large current of 30 A. By elevating the battery voltage, a drastic reduction in motor current ( $0.5 \sim 2$  A) becomes possible and permits a shift from six high current discrete power Metal Oxide Semiconductor Field Effect Transistors (MOSFETs) to single chip micro-inverter ICs. We have successfully developed the record high blocking voltage of 750 V and the largest current capability of 4.5 A micro-inverter IC [3].

Firstly, the concept of high voltage auxiliaries is shown. Then, it is shown the most important technologies in the concept, which are the sensorless sinusoidal wave drive technology and the single chip micro-inverter IC technology. Finally, a test system of high voltage blower motor is driven by using these technologies. It is experimentally assured that the power efficiency of the high voltage test system is higher than that of conventional 12 V system.

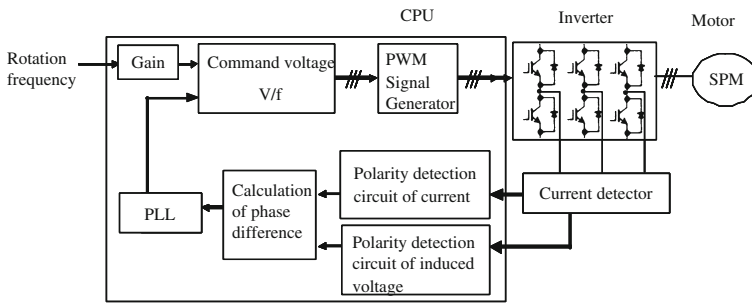
## 2 Concept of High Voltage Auxiliaries

Figure 1 shows a circuit diagram of voltage system. A step down DC/DC converter is used to charge supply currents from the high voltage battery. Up to now, automotive low power electronics operate under a battery voltage of 12 V. By means of elevating supply voltage using high voltage battery, we can achieve better efficiency and reduction of electronic parts.

Figure 2 shows a block diagram of high voltage blower motors. For example, blower fan motors are driven by a large current of 30 A under a 12 V battery. And the electronic circuits are assembled from many electronic parts. On the other hand, under a high voltage of 300 V battery, a drastic reduction using motor current  $\sim 2$  A becomes possible and permits a one-chip high voltage micro-inverter IC.



**Fig. 1** Concept of high voltage auxiliaries. **a** A circuit diagram of voltage system. **b** Electronic parts of inverter in blower motor system



**Fig. 2** A block diagram of blower motor system

### 3 Sensorless Sinusoidal Wave Drive Technology

High power automotive electronics are generally controlled with a sinusoidal waveform current. Typically, they are controlled by vector controlled sinusoidal drives, which require a high performance CPU. In this system, it is not necessary to detect or estimate the rotor position. Figure 3 shows a sensorless sinusoidal wave drive technology. The technology does not require current sensors but can be used to estimate the phase difference between the motor voltage and the motor current by sampling the voltage of shunt resistors. It can maximize the power by controlling the phase difference.

The features of this technology are the simplified control algorithm and the novel detection method of the induced voltage. Figure 4 shows a detection method of induced voltage and motor current at zero vector.

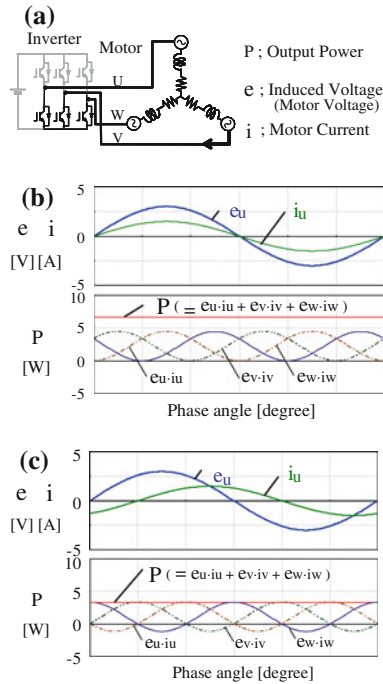


**Fig. 3** A sensorless sinusoidal wave drive technology. **a** A blower motor and a inverter system. **b** Output Power in case that a phase angle of  $e$  is equivalent to that of  $i$ . **c** Output Power in case that a phase angle of  $e$  is NOT equivalent to that of  $i$

### 4 Micro Inverter IC

In the consumer electronics field, micro-inverter ICs up to 500 V 3 A ratings have been developed and widely used [4, 5]. On the other hand in the automotive electronics of HEV/EV, micro-inverter ICs have not yet been used because of the severe requirements related to blocking voltage (BV), current capability, efficiency, temperature, and so on. Even if it takes a BV for example, more than 700 V in all temperature range is required for a HEV application.

Yasuhara et al. reported that his SOI lateral diode achieved the high BV of 650 V by means of introducing interface-N-layer (INL) with  $1.3 \times 10^{12} \text{ cm}^{-2}$  arsenic ion dose on a 3  $\mu\text{m}$ -thick buried oxide (BOX) [6]. Akiyama et al. reported that the higher BV of 1050 V was achieved in his lateral diode fabricated in silicon-on-double-insulator (SODI) structure, which was formed by backside silicon etching of SOI wafer followed by dielectric layer deposition and metal electrode formation [7]. Endo et al. reported that his lateral insulated gate bipolar transistor (LIGBT) with SRFP fabricated in SOI with 2  $\mu\text{m}$ -thick BOX achieved good characteristics not only in the high BV of 580 V, but also in the fast switching of 280 ns [8]. However, there are no reports that a SOI micro-inverter IC

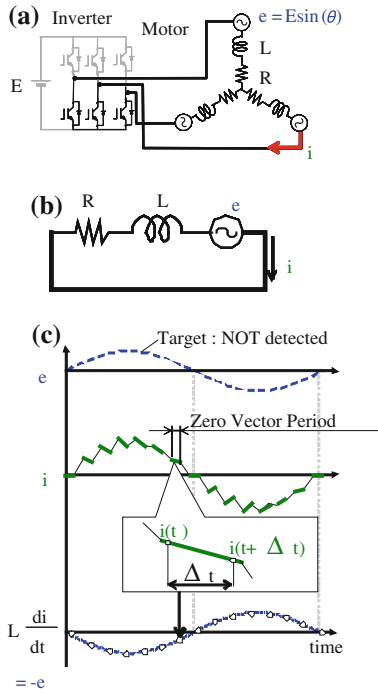
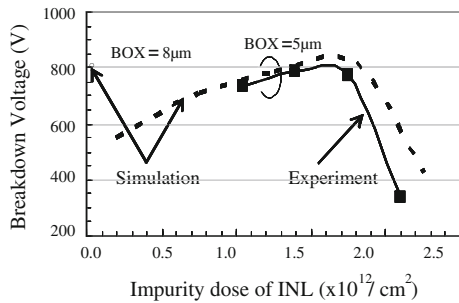


**Fig. 4** A detection method of induced voltage and motor current at zero vector. **a** A switching state at zero vector. **b** Equivalent circuit at zero vector. **c** Link between  $e$  and  $i$  at zero vector

**Fig. 5** Schematic cross-section of SOI micro-inverter IC



achieved a higher BV than 700 V and a larger current capability than 3 A simultaneously.

We have developed the record high BV of 750 V and the largest current capability of 4.5 A SOI micro-inverter IC, which is made possible by the newly developed high voltage reliability technology and high-speed and low-dissipation E<sup>2</sup>LIGBT [9] based on reproducible device design and process sequence.

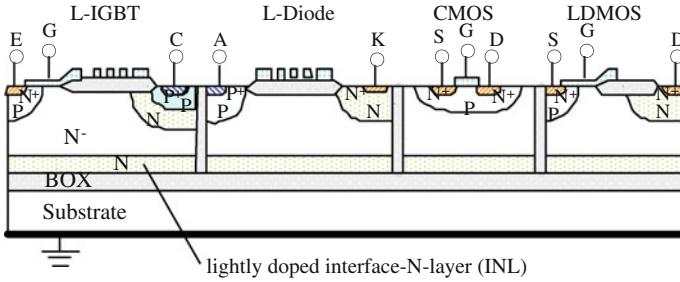
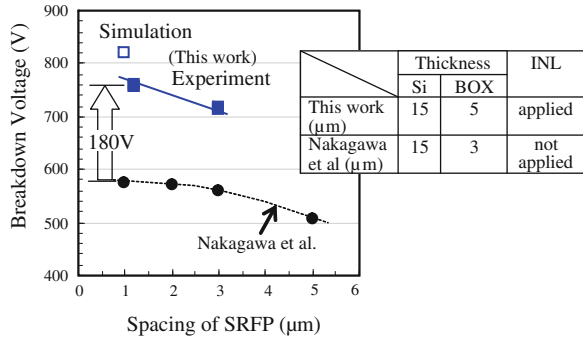


**Fig. 6** Breakdown voltage of SOI lateral devices as a function of impurity dose of INL

**Fig. 7** Schematic electric field reduction structure of SRFP integrated into high-side LIGBT



### 4.1 High Voltage and High Reliability Technology

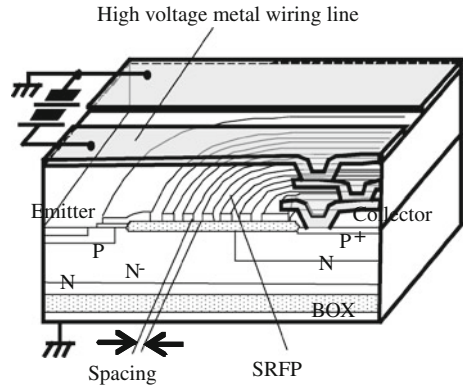
#### 4.1.1 Thinner BOX SOI with Lightly Doped INL

Figure 5 shows schematic cross-section of SOI micro-inverter IC consisting of LIGBT, lateral diode (LDiode), lateral-diffused metal–oxide–semiconductor (LDMOS), and complementary metal–oxide–semiconductor (CMOS). By introducing a lightly doped INL on the BOX film, BV of lateral power devices is considerably improved. Figure 6 shows simulated and measured blocking characteristics of SOI lateral devices. Thickness of the BOX is selected as 5 μm which is the practical limit of bonded SOI wafer. Applying the INL on the BOX, the highest BV is experimentally obtained as 780 V (INL dose:  $1.7 \times 10^{12} \text{ cm}^{-2}$ ) which is comparable to 800 V of 8 μm BOX SOI without INL. The optimized INL dose of  $1.7 \times 10^{12} \text{ cm}^{-2}$  is somewhat larger than  $1.3 \times 10^{12} \text{ cm}^{-2}$  which was previously reported.

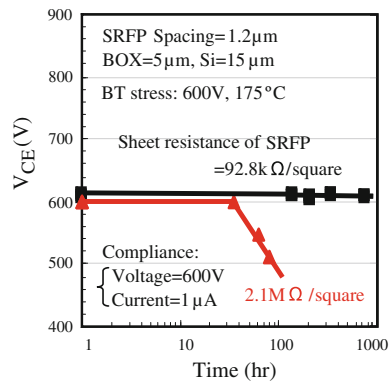
#### 4.1.2 High reliability SOI Technology Over 750 V

Figure 7 shows schematic electric field reduction structure using poly silicon based SRFP. The BV of LIGBTs is influenced by the high voltage metal wiring

**Fig. 8** Breakdown voltage of SOI LIGBTs as a function of SRFP spacing



**Fig. 9** Long-term endurance test of blocking voltage under bias and temperature stress

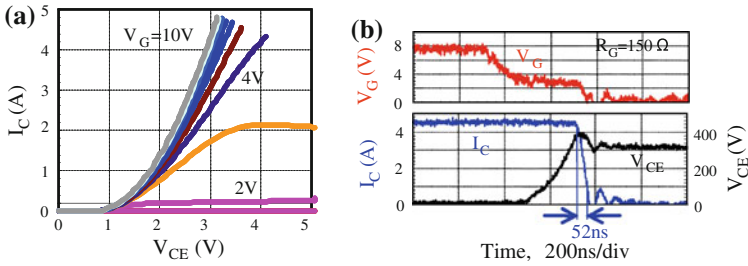


line over the SRFP. It was found that the BV greatly depends on the spacing of the poly-silicon of SRFP.

Figure 8 shows the simulated and measured BV of SOI LIGBT with the poly-Si spacing as a parameter. The highest BV of 760 V is experimentally obtained when the narrow 1.2 μm spacing is adopted. The BV of 760 V is increased by 180 V, compared with the previously reported data. The optimized spacing of 1.2 μm shows that a turbulence of electric field at the silicon surface caused by overlaid high voltage metal wiring can be effectively relaxed by narrowing the spacing of SRFP.

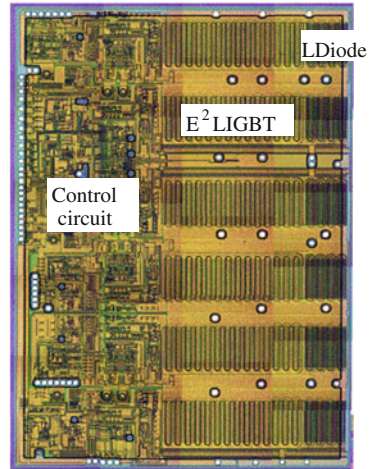
The critical importance in the automotive application is the reliability issue. It has been found, for the first time, that the stable and reliable high blocking voltage of 760 V is assured by controlling the sheet-resistance of the poly-Si layer of the SRFP.

Figure 9 shows the long-term endurance test of blocking voltage under bias (600 V) and temperature (175 °C) stress. Two cases of SRFP poly-silicon sheet resistances,  $R_S$ ,—92.8 kΩ/square (impurity dose:  $2.5 \times 10^{13} \text{ cm}^{-2}$ ) and 2.1 MΩ/square ( $1.2 \times 10^{13} \text{ cm}^{-2}$ )—were evaluated. 92.8 kΩ/square of  $R_S$  is low enough to ensure 1000 h endurance. It has been found that the stability of BV strongly



**Fig. 10** Measured electrical characteristics of fabricated SOI E<sup>2</sup>LIGBT. **a** Static characteristics. **b** transient characteristics

**Fig. 11** Photo of the 750 V 4.5 A SOI micro-inverter IC



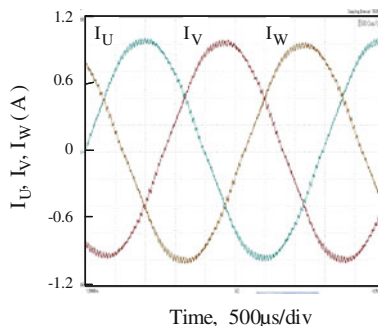
depends on  $R_S$ . The relationship between  $R_S$  of poly-Si and long-term stability of BV is seemed to be related to interface trapped charge density and current through the SRFP.

### 4.2 High-Speed and Low-Dissipation E<sup>2</sup>LIGBT

We have developed and re-optimized the high speed E<sup>2</sup>LIGBT for the high current 4.5 A micro-inverter application [8]. Figure 10 shows measured electrical characteristics of the high current E<sup>2</sup>LIGBT. In Fig. 10a and b,  $V_{ON}$  is considerably as low as 3.1 V at 4.5 A (170 A/cm<sup>2</sup>) and the fall time,  $t_F$ , is remarkably as short as 52 ns.



**Fig. 12** Output current waveforms of the micro-inverter IC driving three-phase brush-less motor



#### 4.2.1 Fabricated IC and Control Circuits

Figure 11 shows photo of the fabricated 750 V 4.5 A SOI micro-inverter IC, which is composed of E<sup>2</sup>LIGBTs, free-wheeling LDiodes, and the control circuits. The control circuits consist of pulse width modulation (PWM) controller, gate drivers, voltage regulators, bootstrap diodes, and so on. The chip size is  $6.2 \times 9.3 \text{ mm}^2$ . In contrast to conventional micro-inverters, which use 30 V 2  $\mu\text{m}$  CMOS, we employed 5 V 0.6  $\mu\text{m}$  CMOS circuits, which make it possible to integrate high level intelligent functions

### 5 Demonstration of Inverter Operation

The test system of a blower motor (250 W 290 V ratings) is successfully driven by the sensorless sinusoidal wave drive technology and the micro-inverter IC as shown in Fig. 12. The experimental conditions are motor speed = 3000 rpm (maximum rating),  $V_{\text{BATTERY}} = 290 \text{ V}$ ,  $I_{\text{BATTERY}} = 0.90 \text{ A}$ , PWM frequency = 20 kHz. Measured input power and power loss in the micro-inverter IC are 261 W and 16 W, respectively. The power efficiency has achieved as high as 94 %, which is at least 10 % higher than that of conventional 12 V blower motor systems. The printed circuit board size reduction has been realized by 40 % by elevating supply voltage from the 12 V voltage battery to the high voltage battery (290 V).

### 6 Conclusions

We have proposed a novel concept of high voltage auxiliaries, which replaces the current 12 V loads with the high voltage loads driven directly by the high voltage battery. And it is assured that the power efficiency of the new test system is as high as 94 %, which is at least 10 % higher than that of conventional 12 V blower motor system.

**Acknowledgments** The authors would like to thank Akio Nakagawa, Norihito Tokura, and Takashi Suzuki for useful discussion, Takeshi Sakai, Shinya Sakurai, and Shogo Ikeura for sample preparation, Yoshitomo Takeuchi and Kazutoshi Shiomi for inverter evaluation. The authors also wish to thank Yasushi Tanaka, Noriyuki Iwamori, and Masahiro Sou for their support throughout this study.

## References

1. Kawahashi A (2004) In: Proceedings of International Symposium. Power Semiconductor Devices and ICs, p 23
2. Rahman K, Anwar M, Schulz S, Kaiser E, Turnbull P, Gleason S, Given B, Grimmer M (2011) SAE Tech Pap Ser, 2011-01-0355
3. Shiraki S, Takahashi S, Yamada A, Yamamoto M, Senda K, Ashida Y, Hiruma A, Tokura N (2012). Jpn J Appl Phys 51(04DP03):1–4
4. Nakagawa A, Funaki H, Yamaguchi Y, Suzuki F (1991) In: Proceedings of international symposium. Power semiconductor devices and ICs, p 321
5. Sakurai K, Maeda D, Hasegawa H (2008) In: Proceedings of international symposium. Power semiconductor devices and ICs, p 323
6. Yasuhara N, Nakagawa A, Furukawa K (1991) IEDM Tech Dig, p 141
7. Akiyama H, Yasuda N, Moritani J, Takanashi K, Majumdar G (2004). In: Proceedings of the international symposium. Power semiconductor devices and ICs, p 375
8. Endo K, Baba Y, Udo Y, Yasui M, Sano Y (1994). In: Proceedings of the international symposium. Power semiconductor devices and ICs, p 379
9. Ashida Y, Takahashi S, Shiraki S, Tokura N, Nakagawa A (2012) Jpn. J Appl Phys 51(04DP02):1–5